

Article

Mapping Plant Functional Types over Broad Mountainous Regions: A Hierarchical Soft Time-Space Classification Applied to the Tibetan Plateau

Danlu Cai ^{1,2,*}, Yanning Guan ¹, Shan Guo ¹, Chunyan Zhang ¹ and Klaus Fraedrich ²

¹ Institute of Remote Sensing and Digital Earth, University of Chinese Academy of Sciences, Beijing, 100101, China; E-Mails: guan@irsa.ac.cn (Y.G.); guoshan@radi.ac.cn (S.G.); zhangcy@radi.ac.cn (C.Z.)

² Max-Planck-Institute for Meteorology, Hamburg, 20146, Germany
E-Mail: klaus.fraedrich@zmaw.de

* Author to whom correspondence should be addressed; E-Mail: caidl@radi.ac.cn;
Tel: +86-10-6487-9961; Fax: +86-10-6488-9570.

Received: 14 February 2014; in revised form: 25 March 2014 / Accepted: 15 April 2014 /
Published: 23 April 2014

Abstract: Research on global climate change requires plant functional type (PFT) products. Although several PFT mapping procedures for remote sensing imagery are being used, none of them appears to be specifically designed to map and evaluate PFTs over broad mountainous areas which are highly relevant regions to identify and analyze the response of natural ecosystems. We present a methodology for generating soft classifications of PFTs from remotely sensed time series that are based on a hierarchical strategy by integrating time varying integrated NDVI and phenological information with topography: (i) Temporal variability: a Fourier transform of a vegetation index (MODIS NDVI, 2006 to 2010). (ii) Spatial partitioning: a primary image segmentation based on a small number of thresholds applied to the Fourier amplitude. (iii) Classification by a supervised soft classification step is based on a normalized distance metric constructed from a subset of Fourier coefficients and complimentary altitude data from a digital elevation model. Applicability and effectiveness is tested for the eastern Tibetan Plateau. A classification nomenclature is determined from temporally stable pixels in the MCD12Q1 time series. Overall accuracy statistics of the resulting classification reveal a gain of about 7% from 64.4% compared to 57.7% by the MODIS PFT products.

Keywords: plant functional types; fast Fourier transform; NDVI time series; Tibetan Plateau

1. Introduction

Plant functional types (PFTs) are groups of plants defined according to several factors, including their functions at organismic level, their responses to environmental factors, and/or their effects on ecosystems [1]. This is particularly relevant for monitoring present state and possible changes in mountainous areas, which “support many different ecosystems and have among the highest species richness globally”. Furthermore, in semi arid and arid regions of the Tibetan Plateau, PFTs play a significant role in biospheric carbon storage and carbon sequestration. Thus it is not surprising that these areas are expected to experience most severe ecological impacts and, therefore, are counted as highly vulnerable [2].

Therefore, reliable information about the geographic distribution of major PFTs in these regions is necessary. Traditional land classifications are biome-based and arbitrary products of the classifying scheme rather than existing natural units [3]. The key distinction between biome *versus* PFT classification is that the latter attempts to unmix mixed pixels. That is, a biome class such as “savanna” needs to be decomposed into proportions of component plant types, grass, broad leaf trees, *etc.* However, representing vegetation by patches of PFTs reduces species diversity in ecological function to a few key plant types whose leaf physiology and carbon allocation are known. Thus analyses of composition and function of ecosystems in a changing environment are possible. This PFT concept has gained favor also amongst modelers, who are trying to predict how vegetation will respond to the effects of climate change.

At present there are three PFT classifications available: (i) Global PFT data sets are obtained from satellite based products; they are produced by the Moderate Resolution Imaging Spectroradiometer (MODIS) Land Team [4]. (ii) PFTs are also extracted from already existing land cover data sets [3,5–8] and, finally (iii) PFTs are derived from Regional Scale Multisource Evidential Reasoning [9], using remote sensing techniques to map higher accuracy regional PFTs. For application to the complex structures of mountainous areas like the Tibetan Plateau these mappings have limitations, as specified below.

PFT products are generated as one of the five MODIS Land Cover products, for which the decision trees classification method is used. Several studies have demonstrated the utility and advantage of decision trees in land cover classification from regional to global scales [10,11]. Moreover, Strahler, Muchoney, Borak, Friedl, Gopal, Lambin and Moody [4] note that the International Geosphere-Biosphere Program (IGBP) classes can be re-labeled or “cross-walked” to provide compatibility with current and future land cover classification systems. However, Sun *et al.* (2008) indicate that the error characteristics (such as magnitudes, spatial and temporal variation) of the MODIS PFT products have not been fully characterized. In addition, detailed information on how to “cross-walk” to the PFT classes are not released [12]. Finally, investigators extracting PFT information from preexisting land cover maps pioneered the development of PFT data sets over broad areas, and still use this method in recent research. However, this PFT information from preexisting land cover maps is predominantly

used in global scale analyses using relatively coarse resolution, and investigators are frequently forced to make assumptions about missing information [7,12]. When several land cover maps are required for producing PFT, compatibility among those maps will be an issue. Moreover, updating such PFT data sets could not be independent from updating land cover maps. (iii) Sun *et al.* (2008) present a method of multisource mapping of PFTs using a suite of MODIS products which improve the overall accuracy and kappa statistic [9]. However, they also note that evidence reasoning could not solve the issue of incorporating regional variations in the spectral and morphological characteristics of PFTs. That is, the method could not obtain a classification procedure for mapping over larger geographic areas (like continents).

Representative information on the time evolution of remote sensing and vegetation data sets can be employed to characterize vegetation types and thereby avoid climate induced phenological shifts. These temporal trajectory analyses are conveniently grouped into four categories [13]: (i) quantifying differences in time series values, (ii) accounting for temporal correlation and non-stationarity, (iii) measuring temporal correlation and, finally (iv) implementing a natural set of harmonic modes. This Fourier mode decomposition is advantageous in areas where human activity is limited, where strong periodicities exist. Thus it could be used to filter non-systematic noise and to separate spatial variations from temporal variability as demonstrated in applications to spectral satellite images or derived vegetation indices and biophysical products (especially Normalized Difference Vegetation Index, see [14–19]).

PFTs in mountainous areas which, to our knowledge, have not been subjected to this analysis technique, is the focus of this study. That is, comprising hierarchical and soft classifications, including digital elevation information, and applying suitable measures of similarity (between candidate pixels and reference types) lead to a novel combinatorial approach to map PFTs in mountainous regions. The methodology, data used and processing procedure is presented in Section 2, followed by an application to the Eastern Tibetan Plateau (Section 3), and a discussion concludes the analysis (Section 4).

2. Methods of Analysis

Datasets and the strategy of improving the PFT classification are introduced in the following. The scheme used in this study is similar as the one used in the standard MODIS PFTs product: evergreen needle leaf trees (ENT), evergreen broad leaf trees (EBT), deciduous needle leaf trees (DNT), deciduous broad leaf trees (DBT), shrub, grass, Cereal crop and broadleaf crop are combined to crop (CC), barren or sparse vegetation (BSV) but without snow and ice (SI), urban and built up types, which are out of scope of the PFTs distribution. For simplicity, the types used will be referred to by their initials.

Three data sets are used as inputs which include five year of half-month data of MODIS NDVI (MOD13A1, 2006 to 2010), five year of annual data of MODIS PFT (MCD12Q1, 2006 to 2010), and the Shuttle Radar Topography Mission (SRTM) elevation data: (i) MOD13A1 data is provided every 16 days at 500-m spatial resolution as a gridded level-3 product in the sinusoidal projection. These are global MODIS vegetation indices, designed to provide consistent spatial and temporal comparisons of vegetation conditions. They are closely related to percent green cover, the fraction of Photosynthetically Active Radiation (fPAR) absorbed by vegetation and, therefore, to gross primary

productivity as demonstrated by satellite-based analyses of land surface vegetation [20–22]. (ii) MCD12Q1, the MODIS Terra plus Aqua 500m resolution Land Cover Type product, incorporates five different land cover classification schemes, derived through a supervised decision-trees classification method. PFT product is generated as one of the five MODIS Land Cover products. The PFT product is used for comparability and training of soft classification determined from temporally stable pixels in the MCD12Q1 time series (temporal resolution of one year). (iii) SRTM is a global digital elevation model (DEM) spearheaded by the National Geospatial-Intelligence Agency (NGA), NASA, the Italian Space Agency (ASI) and the German Aerospace Center (DLR) with 90 meter resolutions for the world [23].

The SRTM dataset in this study is resized according to the spatial resolution of MODIS product by nearest neighbor resampling in ENVI software. Some geostatistical approach would probably generate more accurate outcomes for relief data than nearest neighbor resampling [24]. But considering both efficiency and specific study regions, we choose, instead of geostatistical approach, nearest neighbor resampling. Previous records support that the hierarchical approach, even coupled with coarse DEM information, is effective in increasing the accuracy of vegetation classification over very rugged terrain [25].

The validation datasets are provided by the Vegetation Map of the People's Republic of China (1:1,000,000, field survey, and for simplicity referred to as China Vegetation Map in the following) and by Makehe Forest Region vegetation map (1:50,000, field survey completed in late 2009, see Section 3). The China Vegetation Map [26], completed in late 2007, describes vegetation distributions, including 11 vegetation type groups (such as broadleaf forest), 55 vegetation types (such as temperate deciduous broad leaf trees) and 960 vegetation species (such as pine, spruce, oak and so on), which are usually used as testing data (see, for example, [27,28]).

Fourier transform: The first step of the hierarchical soft classification methodology is to transform the original image time series into frequency domain using fast Fourier transform (FFT, see Equation (1)). Each pixel location in the original image contains a time series, which is a periodic signal. The FFT decomposes the periodic signal into a set of scaled sine and cosine waves that can be summed to reconstruct the original signal and can be used to transform any equidistant discrete time series f_t . The Fourier transformed components of NDVI time series to segment remote sensing hard vegetation types are successfully reported in the previous research (see introduction) and is given by:

$$F(k) = \frac{1}{N} \sum_{t=0}^{N-1} f_t * e^{-\frac{2\pi ikt}{N}} \quad (1)$$

where t is an index representing NDVI layer number; f_t is the t^{th} time series value; k is the number of Fourier component (or harmonic) and N is the total number of layers in the time series. According to Euler's formula $e^{i\theta} = \cos \theta + i \sin \theta$, Equation (1) can be decomposed into a set of cosine (real part) and sine (imaginary part) waves $F(k) = \frac{1}{N} \sum_{t=0}^{N-1} f_t * [\cos(\frac{2\pi kt}{N}) - i \sin(\frac{2\pi kt}{N})]$. The cosine and sine parts, $F_k^R = \frac{1}{N} \sum_{t=0}^{N-1} f_t * \cos(\frac{2\pi kt}{N})$ and $F_k^I = \frac{1}{N} \sum_{t=0}^{N-1} f_t * \sin(\frac{2\pi kt}{N})$ provide amplitude $A_k = \sqrt{F_k^{R^2} + F_k^{I^2}}$ and phase $\phi_k = \arctan(\frac{F_k^I}{F_k^R})$ of each harmonic.

Classification: The classification procedure follows a stepwise hierarchy from broad spatial partitioning to a detailed soft diagnostics, which requires a metric to estimate the similarity between reference and candidate pixels. Similar to a top-down hierarchical classification, we consider a multiple stage process in which broad categories are separated first and finer categories within broad categories are further classified afterwards.

By setting a threshold value for the amplitude A_0 we define broad categories (threshold values are set according to the mean, standard deviation, and especially standard error of the five-year NDVI average, details in Section 3). A_0 represents the amplitude of the average NDVI, which is closely related to the biomass information of land surface vegetation [29]. Similar amplitude A_0 types are separated first as broad categories and detailed PFTs within broad categories could be further separated by different phenological and elevation information.

The soft classification satisfies characteristics of PFTs which (compared with hard classes, such as “savanna”) are proportions of component of plant types, grass, broad leaf trees, *etc.* Transforming input time series into partitioning frequency regions is a critical step for combining similar integrated NDVI and phenological information. Due to its generality, the theory of transforming and partitioning does not specify how to compute similarity measures of PFTs by preserving their soft attributes. Therefore, soft classification is introduced in this study to enable a better mapping behavior of land surface PFTs, particularly regarding points that are challenging because they lie on transition or mixed zones [30]. In summary, soft PFT similarity measures are implemented following the three subsequent steps.

Step-1: Extraction of persistent PFT pixels: Traditional reference selection requires ground truth or visual interpretation, but which are untypical for the 500 m resolution MODIS products. Our reference selection considers pixels (from 2006 to 2010 MODIS PFTs products) which consistently belong to the same PFT over the 5-year period to be representative. The persistent pixels of each PFT selected in this step are used as a mask to generate mean reference vectors of each PFT in the next step.

Step-2: Reference vectors for individual PFTs: In this paper, each pixel is referred to as a candidate pixel, containing the same number of values as number of layers. A vector is introduced for each candidate pixel to record those values. Thus, the dimension of a vector equals to the number of layers. Among candidate pixels, those for reference are persistent pixels selected from Step-1. A reference vector is a mean vector including a set of mean values, each of which represents a mean of a particular PFT in a input layer, such as amplitude A_K , phase PHI_K and elevation. The mean value for each layer is computed by first summing all data value of the pixels corresponding to a PFT, and then dividing the sum by the number of pixels in that mask. For example, suppose we select the first 15 amplitudes A_K and phases PHI_K , include digital elevation data and the amplitude A_0 , we obtain 32 layers; that is, the dimension of a mean vector for each PFT yields 32.

Step-3: Similarity measure: The distance from each candidate vector to this mean vector of each PFT class (i) for each layer is calculated as:

$$d_i = \sqrt{\sum_{layer} [(PV_{x,y,layer} - MEAN_{i,layer})]^2} \quad (2)$$

where $PV_{x,y,layer}$ is the pixel value at location (x,y) on a particular layer; $MEAN_{i,layer}$ is the mean value in a PFT mask on the same particular layer. In this way, each PFT is defined by a mean reference vector. The distance metric is a scale insensitive metric which will not be over dominated by large range layers, such as A_0 and the digital elevation model, due to subtracting a mean PFT vector in associated spatial partitioning regions. The measure of similarities between a mean reference vectors and candidate vectors are based on normalized distances (Equation (3)):

$$normalized(X_i) = \frac{1}{d_i} * \frac{1}{\sum_{layer} \frac{1}{d_i}} \quad (3)$$

where d_i is the distance of a candidate pixel from the mean vector of a PFT class i ; $normalized(X_i)$ is an index describing the candidate pixel belonging to class i by converting distance i to scale 0~1. If the vectors are identical (the d_i in Equation (2) is 0), in this case, in such a case the normalization of Equation (3) is assumed to return 1.

3. Application of the Hierarchical Soft Classification: Results for Eastern Tibet

The eastern Tibetan Plateau (Figure 1) covers a large part of the Eurasian continent (25°N to 38°N, 88°E to 105°E); it comprises topographically, biologically and climatically complex areas. The elevation ranges from 120 m to more than 7200 m and the average altitude is about 3900 m. Several major rivers originate there, including the Yanu Zangbo River, Lancang River, Nu River, Yellow River, Yangtze River, Dadu River, Min River and Jialing River. Biologically, due to the integrated influence from latitudinal, longitudinal and altitudinal zonality, land cover types show a rich diversity (Figure 1). However, the Tibetan Plateau not only has unique climatic conditions and physical environment, but is also sensitive to global change, which makes a very fragile environment for vegetation growth. Climatically, high altitudes are associated with relatively low temperatures and very strong gradients [31]. It contains five provinces of China, including the whole Qinghai province, part of Xizang (Tibet), Sichuan, Gansu and Yunnan provinces.

Suitably employing the tools introduced in the previous section provides a two level hierarchical classification scheme to stratify eastern Tibetan Plateau into smaller mapping categories and to describe detailed variation of PFTs within smaller mapping categories.

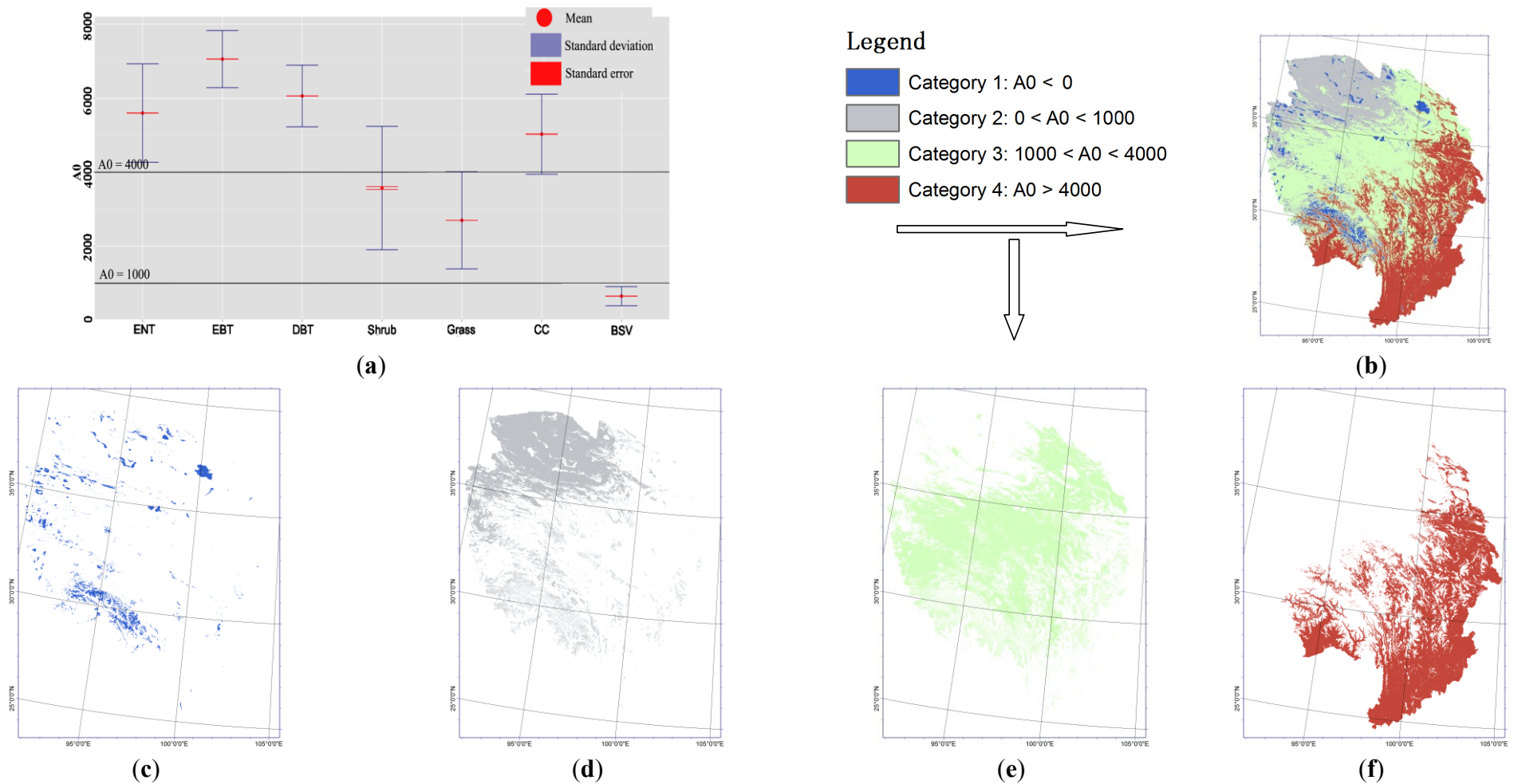
First level classification (Fourier transform and spatial partitioning): After Fourier based decomposition, we define four broad categories (as first level) by setting thresholds for the amplitude A_0 according to the mean, standard deviation, and especially standard error of each PFT: Water or snow and ice (category1, $A_0 < 0$), these type are is should to show no vegetation, that is, the average $NDVI \sim A_0$ is supposed to be below 0; barren or sparse vegetation (category2, $0 < A_0 < 1000$); grass and part of shrub (category3, $1000 < A_0 < 4000$); the rest (category4, $A_0 > 4000$) with five types (see Figure 2a). Generally, standard deviation is a measure of dispersion within a data set whereas standard error is considered to be the level of error (dispersion) of the data from a population mean. Therefore, standard error in Figure 2a indicates that each PFT sample is representative for a population. Besides standard error, Table 1 presents accuracy assessment using random points for the four categories. The producer's and the user's accuracies for the four categories are used to support the selected threshold. Figure 2b–f shows the spatial partitioning results according to the setting of

threshold values, which are generated to keep the detailed PFTs mapping from being dominated by large range layers such as A_0 .

Figure 1. Geographical setting of eastern Tibetan Plateau (China) including five provinces of China: Qinghai province, part of Xizang (Tibet), Sichuan, Gansu and Yunnan provinces. Several major rivers originate there, including the Yanu Zangbo River, Lancang River, Nu River, Yellow River, Yangtze River, Dadu River, Min River and Jialing River.



Figure 2. Spatial partitioning (first level of hierarchical soft time-space classification): **(a)** illustration of the mean standard deviation and standard error of amplitude A_0 for each PFT; **(b)** four broad mapping categories segmented by amplitude thresholds A_0 ; **(c)** category1 with non-vegetation; **(d)** category2 with barren or sparsely vegetated; **(e)** category3 includes shrub or grass; **(f)** category4 includes the remaining five types. Vegetation types represented by initials: evergreen needle leaf trees (ENT), evergreen broad leaf trees (EBT), deciduous needle leaf trees (DNT), deciduous broad leaf trees (DBT), crop (CC), barren or sparse vegetation (BSV).



Second level classification: The following second level of hierarchical classification employs data from the Eastern Tibetan Plateau on the step-by-step basis introduced above.

(i) *Selection of reference (persistent) samples* for supervised classification is commonly accomplished in three ways by (1) ground truth observation, (2) visual interpretation of the observed image and (3) using higher spatial resolution satellite images. Reference samples from ground truth of complex topography (like the eastern Tibetan Plateau, lat \times long $\approx 13 \times 17$ degrees) are untypical. Likewise, visual interpretation of NDVI time series (including the digital elevation information) is uncommon, if only the inputs of this study are used; finally, reference samples selected from higher spatial resolution satellite images often require a too sophisticated data fusion process. Therefore, a novel procedure is introduced to obtain reference samples for complex mountainous regions, which is flexible, robust and easy to apply: Assume that the accuracy of those pixels persistently belonging to the same PFT in five years is sufficiently high to represent the unique pattern of a distinct PFT. Then data fusion is not necessary because both of the two products (MODIS PFT and MODIS NDVI) share the same spatial resolution, coordinate system, and even satellite. In addition, smoothing by spatial averaging (Section 2) enhances the ability for reference samples to provide a distinct and representative PFT. It appears that, among the selected pixels, none of them belongs to Deciduous Needle leaf trees. Therefore, it will not be considered in the detailed PFTs mapping process in the following case study. The remaining five or seven PFTs are taken as examples, which are represented in terms of their most relevant Fourier harmonics and by their living elevation situation (Figure 3).

The following points are noted: (i) Harmonic mode represents complete cycles over the five-year time series. That is, the annual cycle shows large amplitude A_5 (Figure 3a). (ii) Vegetation elevation attributes (Figure 3c) the altitude living order for PFTs from high to low levels: evergreen needle leaf > deciduous broadleaf tree > evergreen broad leaf tree. (iii) Annual, semi-annual and one-third annual crop modes are represented by the 5th amplitude component, the 10th amplitude component and in the 15th amplitude component, separately (Figure 3g–i). (iv) The phase information shows a large variability for each PFT, representing the large inter-annual fluctuation in the phenological profile of a specific PFT (due to different climatic condition in different parts of the study area).

(ii) *Reference mean vectors (and representative layers)* are selected according to their ability to discriminate different PFTs. First, integrated NDVI, amplitude A_0 , contains information about the time mean characteristics of different PFTs. For example, in long time series the integrated NDVI of evergreen broadleaf tree (Category4 in Figure 2a) is greater than of deciduous broadleaf tree. Next, the amplitudes of the annual, semi-annual and one-third annual modes provide support for discrimination of PFTs (see standard error, the level of dispersion, in Figure 3); for this study area, the semi-annual vegetation mode appears to be sufficient. Finally, the digital elevation model can also improve the accuracy of PFTs mapping, because each PFT may show a distinct upper and lower limit of plant growth. Now, a reference spatial average for each PFT is determined from all representative layers; the phase information is not considered due to the large spatial and/or inter-annual variability of each PFT.

(iii) *The similarity measure* is based on the differences of integrated NDVI, phenological and altitudinal behavior between a reference mean vector of each PFT compared with the candidate vectors using the normalized distance (Equation (3)). Two vectors of better match in all layers have a greater normalized distance value. It is worth noting that the study area is divided into four categories where

potential vegetation type is different as demonstrated by the normalized distance of PFTs (Figure 4, note that Category2 is assigned into a single Type, Category1 is out of the scope of vegetation classification, thus, both of them are not shown).

Figure 3. Mean and standard deviation of each PFT in (a) amplitude A_5 ; (b) Phi_5 ; and (c) DEM; Mean and standard deviation of different crops in (d) A_5 ; (e) A_{10} ; (f) A_{15} . For simplicity, vegetation types represented by their initials: evergreen needle leaf trees (ENT), evergreen broad leaf trees (EBT), deciduous needle leaf trees (DNT), deciduous broad leaf trees (DBT), crop (CC), barren or sparse vegetation (BSV), annual crop (C_1), semiannual crop (C_2), third annual crop (C_3). The amplitudes peak of the annual, semi-annual and one-third annual modes provide support for discrimination of PFTs (see arrows)

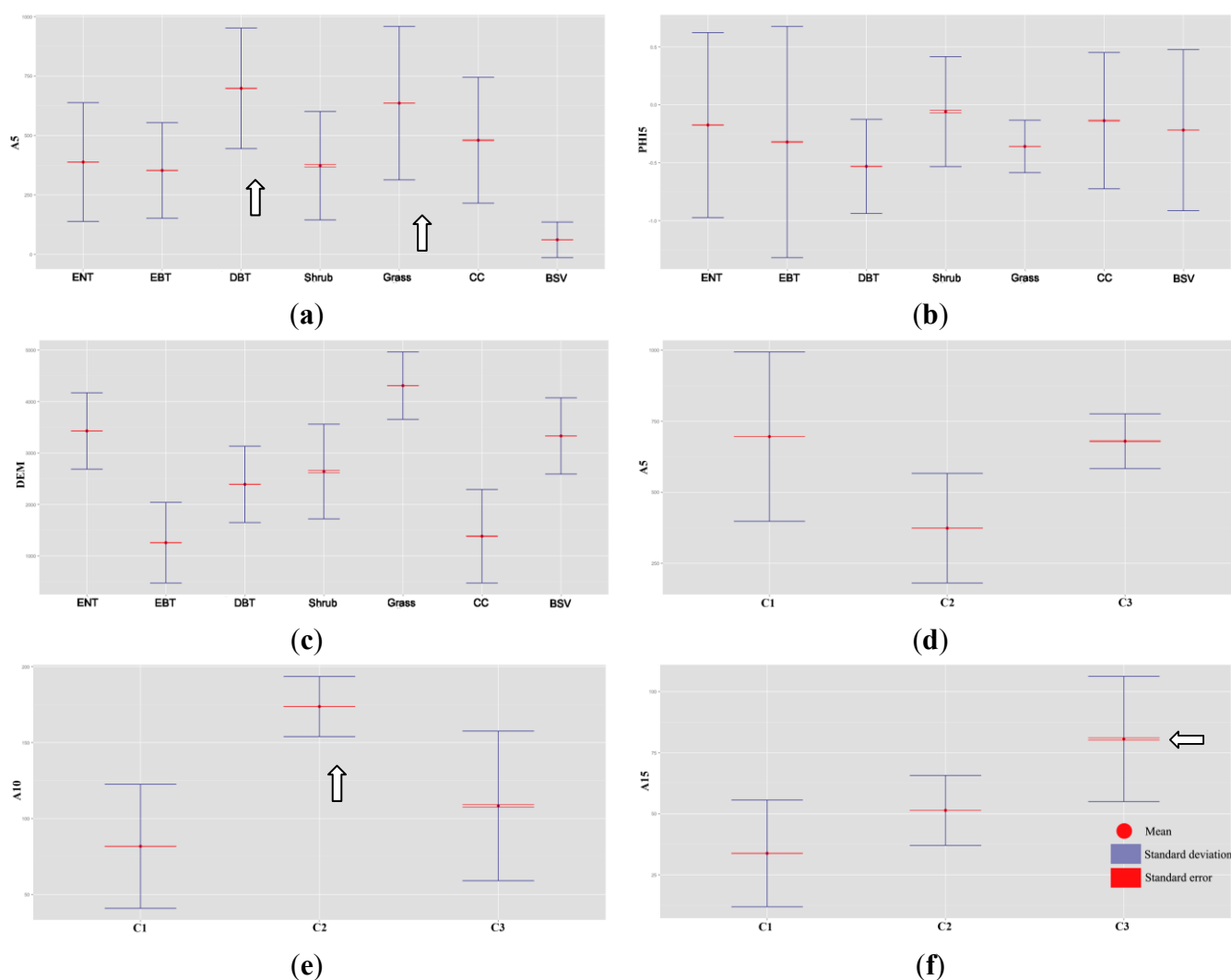


Figure 4. Normalized distance between reference mean vector and candidate pixels of Category4: (a) evergreen broad leaf trees; (b) evergreen needle leaf trees; (c) deciduous broad leaf trees; (d) shrub; (e) cereal crop and (f) broad leaf crop in category4; (g) grass and (h) shrub.

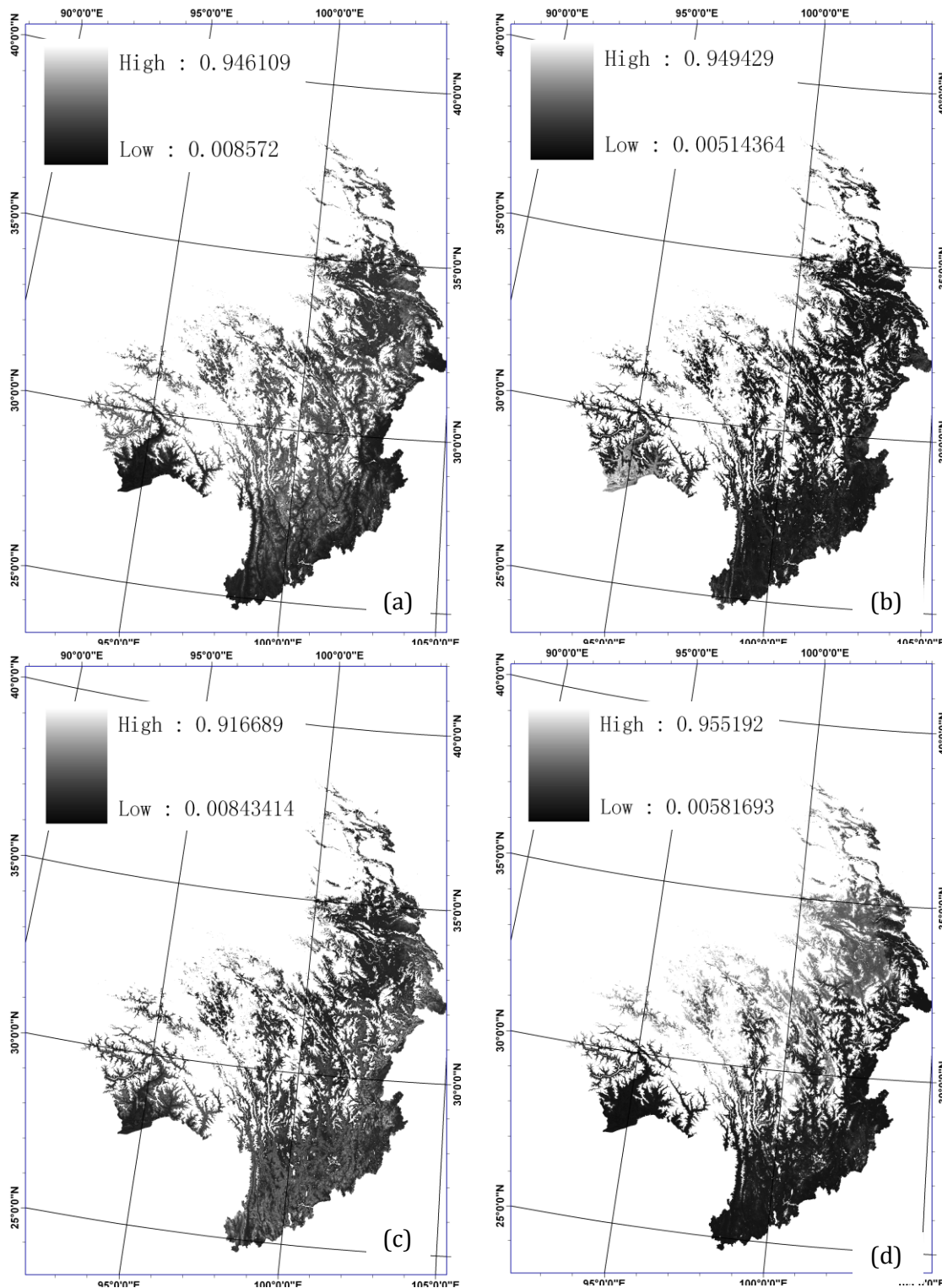
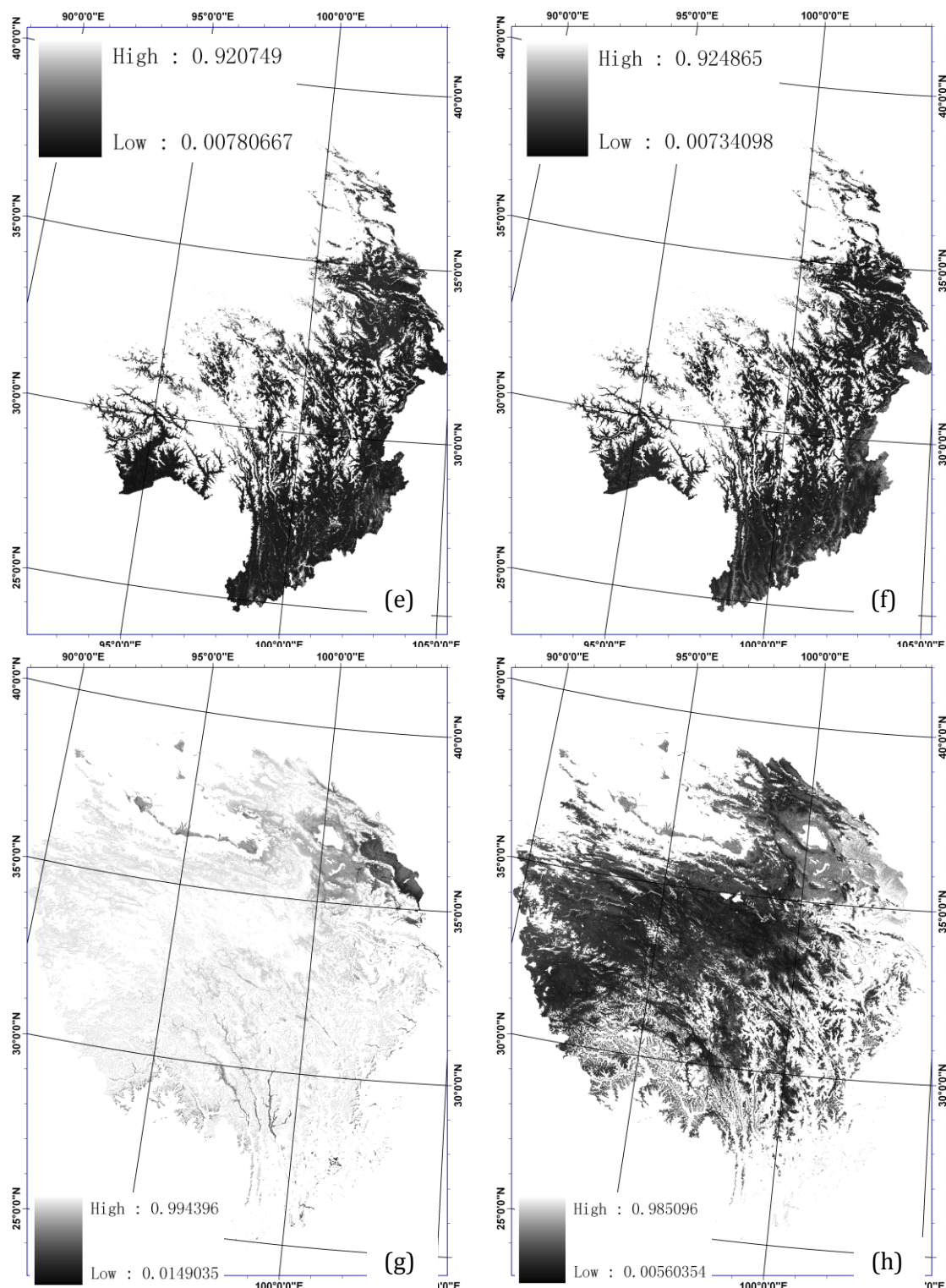


Figure 4. Cont.



Assessment and visualization: The similarity measure calculates soft PFT results, which are proportional components of plant types. Accuracy assessment requires additional interpretation to pass from these soft PFT results to a hard classification map. Thus we assign a pixel with the greatest normalized distance to the PFT (hereafter refer to hardened classifications) just in the interest of showing the spatial distribution of dominant PFTs and a better comparability between the MODIS product and this PFT results. Figure 5a shows hardened classifications and Figure 5b shows the

MODIS 2007 PFT product. Figure 6 is a highlight comparison of vegetation distribution from Makehe Forest Region located in Sanjiangyuan Nature Reserve. To be comparable, closed/open forest and closed/open shrub of the 1:50,000 field survey are combined to forest (green), shrub (yellow) and others (white), as well as results from hierarchical soft time-space classification and MODIS (see Figure 6). Besides a visual comparison of vegetation maps, a statistical approach is also applied to compare classification to field data in order to evaluate accuracy. Tables 1 and 2 summarize the hierarchical classification result and the MODIS 2007 PFT products compared with reference points from the China Vegetation Map. A total of 13,081 reference points were selected from the China Vegetation Map using the proportionate stratified random method with a minimum sample size of 100. Classification accuracies include producer's and user's accuracy and kappa statistics. Furthermore, we employ a spatial pixel-by-pixel comparison between MODIS PFT products and our hierarchical soft time-space classification scheme (Table 3).

To make the overall approach better validated and more comprehensible, a flowchart (Figure 7) and statistics of vegetation coverage in Makehe Forest Region are provided (Table 4).

Figure 5. Comparison of (a) phenological hierarchical classification and (b) MODIS 2007 PFT for eastern Tibetan Plateau. Vegetation types represented by initials: evergreen needle leaf trees (ENT), evergreen broad leaf trees (EBT), deciduous needle leaf trees (DNT), deciduous broad leaf trees (DBT), shrub, grass, crop (CC), snow and ice (SI), barren or sparse vegetation (BSV).

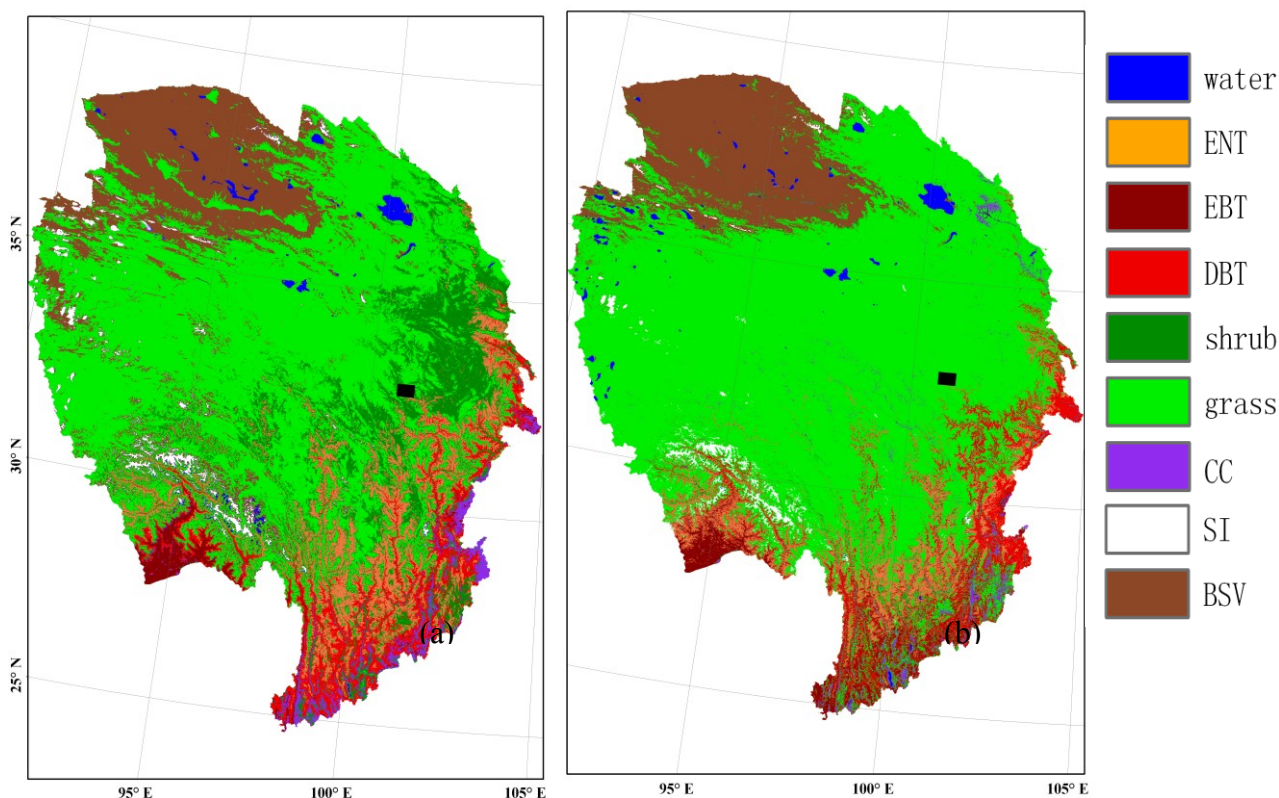


Figure 6. Vegetation distribution map from Makehe Forest Region located in Sanjiangyuan Nature Reserve: (a) 1:50,000 field survey; (b) hierarchical soft time-space classification; and (c) MODIS 2007 PFT product. Note that, closed/open forest (green) and closed/open shrub (yellow) of the 1:50,000 field survey is combined for a better comparison; related statistics are provided in Table 4.

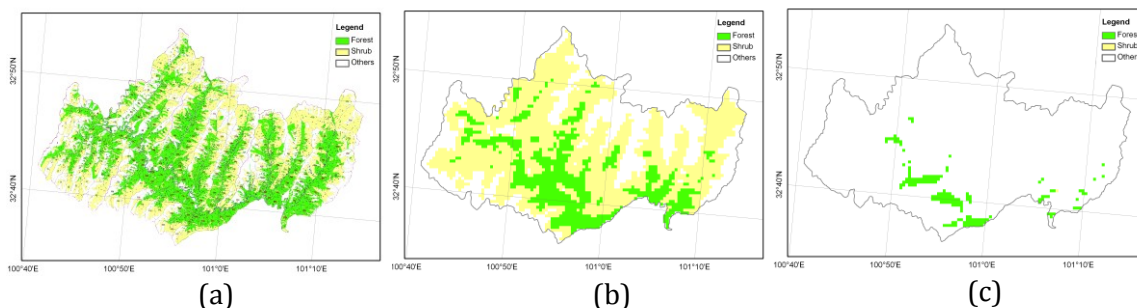
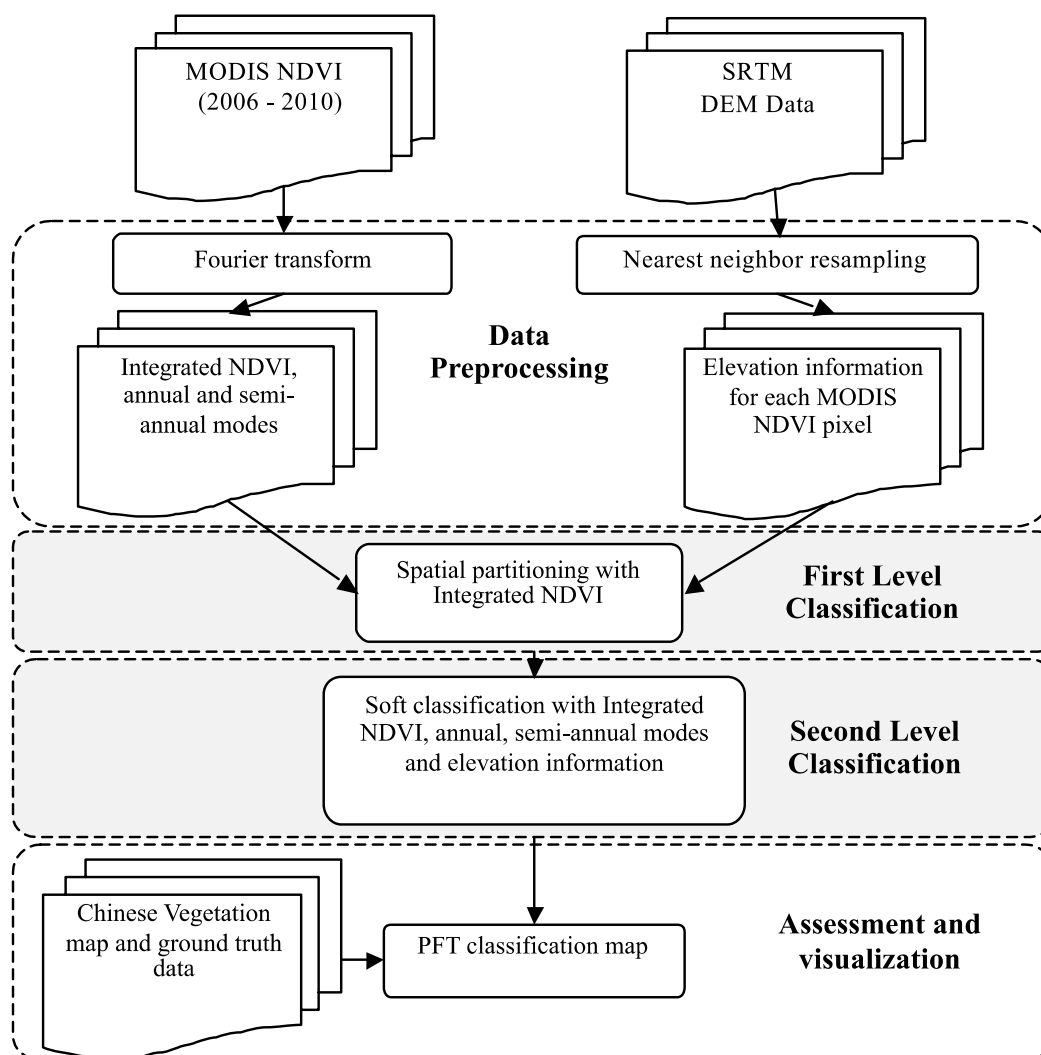


Figure 7. Flowchart of the overall approach applied in Tibetan Plateau.



Comparison and discussion: Our hierarchical soft classification scheme is applied to map PFTs in a complex terrain environment (spanning a height of more than seven kilometers) and compared with the classical MODIS PFT product. The following results are achieved.

(i) *Hierarchical soft classification scheme:* The confusion matrix (Table 1) shows the accuracy of both the first level coarse categories and the detailed PFTs results (based on 13,081 reference points selected from China Vegetation Map). The producer’s (user’s) accuracies of the coarse categories are 63.06%, 92.84%, 64.60%, 69.61% (69.14%, 59.27%, 83.61%, 59.15%), respectively. The accuracy of detailed PFTs results could have been improved by improving the accuracy of the coarse categories. However, we set threshold values according to the mean and standard deviation of the five-year average $NDVI \sim A_0$ to keep the scheme generally applicable.

Table 1. Confusion matrix of the hierarchical soft classification map: aggregated (the four broad categories) and detailed (plant functional types) accuracies are shown below (based on 13,081 reference points selected from Chinese Vegetation Map). For simplicity, vegetation types represented by initials in bracket: evergreen needle leaf trees (ENT), evergreen broad leaf trees (EBT), deciduous needle leaf trees (DNT), deciduous broad leaf trees (DBT), shrub, grass, crop (CC), snow and ice (SI), barren or sparse vegetation (BSV).

Research	TRUE	Zone1		Zone2	Zone3		Zone4			User’s Accuracy		
		Water	SI	BSV	Grass	ENT	EBT	DBT	Shrub		CC	
Zone1	Water	42.11	4.92	0.27	0.16	0.11	0.00	0.00	0.38	0.00	77.86	69.14
	SI	18.73	78.22	0.25	0.74	0.05	0.00	0.00	0.74	0.00	51.15	
Zone2	BSV	23.94	14.75	92.84	16.77	0.37	0.17	1.00	3.18	2.04	59.27	59.27
Zone3	Grass	10.42	2.11	6.39	64.70	13.27	3.78	19.00	35.15	67.01	83.61	83.61
	ENT	0.14	0.00	0.02	0.67	41.04	17.56	27.00	10.37	3.74	52.27	
	EBT	0.14	0.00	0.00	0.02	0.32	45.96	1.00	0.31	12.59	81.16	
Zone4	DBT	0.00	0.00	0.00	0.24	15.62	25.65	41.00	3.61	7.14	5.86	59.15
	Shrub	4.51	0.00	0.23	16.77	29.05	5.16	10.00	45.90	2.38	33.54	
	CC	0.00	0.00	0.00	0.03	0.16	1.72	1.00	0.36	5.10	30.61	
		42.11	78.22	92.84	64.60	41.04	45.96	41.00	45.90	5.10		Overall Accuracy =
Producer’s Accuracy			63.06	92.84	64.60			69.61				64.42%
												Kappa Coefficient =
												0.47

Detailed classification, which employs the soft similarity measure by combing Fourier components and elevation model, groups the pixels in proportional relation to the vegetation types and thus provide a higher accuracy than MODIS PFT products (see from Tables 1 and 2). For almost all vegetation types this yields a close relation to the China Vegetation Map (field survey), especially for PFTs in high integrated NDVI regions ($A_0 > 4000$). For example, the producer’s accuracy increases (in absolute terms) by 3.27%, 20.60%, 17.77%, and 27.6% for evergreen needle leaf trees, evergreen broad leaf trees, deciduous broad leaf trees, and shrub, respectively. For user’s accuracies,

the maximum improvement occurs for the evergreen broad leaf trees increasing from 42.77% (MODIS 2007 PFT products) to 81.16% (our hierarchical soft classification). The overall accuracy achieved increases from 57.68% (MODIS 2007 PFT products) to 64.42% (research result), with the Kappa Coefficient improving by 0.1. Note that Water and Snow are not included as a PFT and therefore not considered for comparison with MODIS.

Table 2. Confusion matrix of MODIS 2007 PFT map (based on 13,081 reference points selected from Chinese Vegetation Map). For simplicity, vegetation types represented by initials in bracket: evergreen needle leaf trees (ENT), evergreen broad leaf trees (EBT), deciduous needle leaf trees (DNT), deciduous broad leaf trees (DBT), shrub, grass, crop (CC), snow and ice (SI), barren or sparse vegetation (BSV).

TRUE MODIS	Water	SI	BSV	Grass	ENT	EBT	DBT	Shrub	CC	Users' Accuracy
Water	44.29	0.00	0.22	0.05	0.22	0.00	0.00	0.07	0.29	89.51
SI	0.69	71.12	0.17	1.27	0.33	0.00	0.00	1.30	0.00	45.08
BSV	26.64	8.02	90.74	13.59	0.06	0.00	0.00	1.17	1.17	54.84
Grass	17.3	19.25	7.58	72.82	21.50	7.68	35.35	54.8	46.20	72.14
ENT	1.73	0.53	0.11	1.94	37.77	32.5	23.23	14.15	7.02	44.93
EBT	0.35	0.00	0.00	0.28	4.29	25.36	1.01	1.74	9.94	42.77
DBT	1.38	0.00	0.06	0.73	14.32	23.57	23.23	7.06	11.11	3.15
shrub	6.57	1.07	1.01	8.84	19.55	9.82	11.11	18.3	13.74	29.89
CC	1.04	0.00	0.11	0.49	1.95	1.07	6.06	1.41	10.53	20.81
Producer's Accuracy	44.29	71.12	90.74	72.82	37.77	25.36	23.23	18.3	10.53	Overall Accuracy = 57.68% Kappa Coefficient = 0.37

(ii) *MODIS PFT scheme*: A pixel-to-pixel comparison between the hierarchical soft classification result and the MODIS 2007 PFT product is also calculated (Table 3). Confusion matrix shows how vegetation types are transferred from MODIS product to this hierarchical classification by adopting the classification procedure in Section 2; that is, 60.80% of the MODIS 2007 PFT product matches the hierarchical classification result. Grass and sparse vegetation types show high consistency. Geographical comparison between the hierarchical soft classification result and the MODIS 2007 PFT product is shown in Figure 5. More spatial details achieved by using the hierarchical classification compared to the MODIS 2007 PFT product, such as regions around latitude 30°~35° and regions near the boundaries of lakes and permanent glaciers. The barren or sparse vegetated type appears in regions near the boundaries of lakes and permanent glacier, which may be attributed to the seasonal change of the lake area or level and to the melting of non-permanent snow and ice.

Table 3. A pixel-by-pixel comparison based on confusion Matrix between this hierarchical soft classification result and MODIS 2007 PFT products. For simplicity, vegetation types represented by initials in bracket: evergreen needle leaf trees (ENT), evergreen broad leaf trees (EBT), deciduous needle leaf trees (DNT), deciduous broad leaf trees (DBT), shrub, grass, crop (CC), snow and ice (SI), barren or sparse vegetation (BSV).

MODIS Research	Water	ENT	EBT	DBT	Shrub	Grass	CC	SI	BSV	User's Accuracy
Water	58.42	0.05	0.00	0.00	0.02	0.02	0.00	5.09	0.53	70.41
ENT	0.04	47.82	12.89	27.24	14.30	2.12	5.95	0.00	0.00	49.57
EBT	0.01	2.58	41.79	6.02	0.14	0.01	0.34	0.00	0.00	61.71
DBT	0.03	20.60	38.92	53.40	3.99	1.19	8.24	0.00	0.00	39.19
Shrub	0.18	12.74	1.17	1.93	29.00	23.66	18.35	0.00	0.00	18.48
Grass	3.01	13.18	1.27	1.44	46.63	64.87	47.35	4.23	15.11	77.95
CC	0.03	1.36	3.94	9.97	1.73	1.04	19.76	0.00	0.02	16.31
SI	31.89	0.17	0.00	0.00	0.16	0.19	0.00	53.43	0.79	65.35
BSV	6.39	1.51	0.02	0.00	4.04	6.89	0.01	37.24	83.56	74.22
Producer's Accuracy	58.42	47.82	41.79	53.40	29.00	64.87	19.76	53.43	83.56	Overall Accuracy = 60.80% Kappa Coefficient = 0.45

(iii) *Field survey evaluation:* The total area of Makehe forest region is 101,602 hm². The forest area itself comprises 23 385 hm² [32]. Therefore, the forested area (non-forest area) accounts for 23.02% (76.98%) of the total area. Statistics of vegetation coverage as well as related comparisons among the hierarchical soft time-space classification result, MODIS 2007 product and field survey records applied in Makehe Forest Region are provided (Table 4). It is noted that, in the aspect of forest coverage percentage, the hierarchical soft time-space classification improves PFTs mapping accuracy in high mountains regions compared to MODIS product.

Table 4. Comparisons of vegetation coverage (in percent) among the hierarchical soft time-space classification result (achieved result), MODIS 2007 product and field survey records applied in Makehe Forest Region.

	Achieved Result	MODIS Product	Field Survey
Makehe	Forest 21.38%	6.61%	23.02%
	Non-forest 78.62%	93.39%	76.98%

Generally, the overall idea of spatial partitioning is to reduce the variability of the average NDVI $\sim A_0$ so that similarity measure is not dominated by large range layers. Phase information is neglected to assure this procedure to be robust enough for bypassing inter-annual phenological variations within a specific PFT due to regions dependent climatic condition. Neglecting phase information is also the solution for the problem mentioned by Sun *et al.* (2008) that evidence reasoning could not solve the issue of incorporating regional variations in the spectral and morphological

characteristics of PFTs [9]. Spatial averages of persistent pixels selected from five year MODIS PFT product are representative to show the unique pattern of each distinct PFT. A soft similarity measure between a candidate vector and an average vector is suitable for the mixed pixel problem, which lies at the heart of the PFT philosophy.

These statistics reveal that the hierarchical soft time-space classification improves the accuracy for most of PFTs, especially in types with higher NDVI values (e.g., Category4, see pixel-to-pixel comparison). That is, for complex mountainous terrain the hierarchical soft classification scheme (based on freely downloadable data) provides PFT maps of higher accuracy (compared to MODIS products) and can be applied to larger areas (compared to the multisource evidence reasoning scheme). In addition, the barren or sparse vegetated type appears in regions near the boundaries of lakes and permanent glaciers. This suggests that the hierarchical soft classification may provide a tool to monitor lake areas or levels changes and the depiction of snow lines. It should also be noted that the PFT maps presented in this paper are generated at the regional level, whereas the MODIS PFT is a global product.

There are limitations and, therefore, scope for future research: (i) Fourier based techniques are advantageous when strong periodicity exists in the temporal series and for filtering non-systematic noise [9]. However, Fourier decomposition may be less appropriate and perhaps alternatives methods (e.g., wavelets) need to be explored, if abrupt changes occur. Piao *et al.* [33] use a Morlet Wavelet Function to detect vegetation change in the same region, but it shows less abrupt changes occurring in our study region which supports Fourier based techniques to be used in this study region using a 5-years time series. Further research will compare both Fourier and wavelet techniques to provide a map in areas where the Yak-Pica-pasture degradation problem persistently arises and in areas where these deleterious dynamics arise in non-persistent regions. (ii) Data and method: Initial studies have used integrated NDVI values to estimate biomass production through the fAPAR [29]. But the relationship between NDVI and biomass can be problematic in some cases, and some other vegetation index could be superior to NDVI, especially at high fAPAR values [34] which requires further analysis in future research. EVI has been developed with exactly this limitation in mind and thus would be an arguably more appropriate index over large and diverse regions. In this study, we use a primary integrated NDVI segmentation and assisting phenology and elevation information to avoid the NDVI saturation problem. For further improvement detailed classification may be necessary, enhancing the accuracy of spatial partitioning and including other appropriate input data sets (for example, adding Leaf Area Index (LAI) data and/or biomass map). However, due to the accuracy and the spatial resolution (1000 m) of MODIS LAI data, we have not used it in this study. Three distance measures have been applied to Fourier based techniques, which combine amplitudes and phases in one equation [13]. Besides that, three other similarity measures are mentioned and compared for detailed vegetation classification, see [35,36]. The simple and effective Euclidean distance employed in this study makes the combination of amplitude and phase information more flexible, even elimination of phase information. A further comparison between NDVI and EVI time series and between different distance measures may be required. (iii) Accuracy statistics: The accuracy statistic provided in this study relates to dominant classes only but soft classifications can, by definition, be more accurate than hard classifications [37]. For example, large (sub-pixel) areas of bare ground in the Tibetan grasslands might be completely undetected in biome (hard) classifications.

4. Conclusion

Quantitative measures of global distributions of vegetation coverage, vegetation type and vegetation change are available from satellite-based data sets and analyses, which have the advantage that they are spatially extensive and temporally frequent. Using remote sensing techniques to map PFTs is a relatively recent field of research. High mountainous regions, which are usually regarded as an ideal area to study the response of natural ecosystems to global climate change, are usually lacking observed vegetation data due to the harsh physical environment. In this paper we introduce a novel technique to map plant functional types over broad mountainous regions. It is based on a two-step hierarchical soft classification strategy to gain plant functional types, including evergreen needle leaf trees, evergreen broad leaf trees, deciduous broad leaf trees, shrub, grass, crop, and sparse vegetation and barren. The first level of segmentation (spatial partitioning) obtained by Fourier decomposition (FFT) of the five-year (2006–2010) MODIS NDVI time series provides the average NDVI $\sim A_0$. On the second level, further FFT modes and the elevation data are employed to obtain detailed proportional PFTs distribution using soft similarity measures. Finally, accuracy assessment leads to an additional interpretation to pass from those proportional PFTs to a hard classification map is introduced. Statistics reveal a gain on overall accuracy (13,081 random samples) by about 7% from 64.4% compared to 57.7% by the MODIS PFT products.

Acknowledgement

Support by the Chinese Science Database (XXH12504-1-12), 135 plan project of Chinese Academy of Sciences (Y3SG0500CX) and the Joint CAS-MPG PhD-Program, by the Max Planck Fellow Group (KF), and the hospitality of the KlimaCampus, University of Hamburg, are gratefully acknowledged (DL). Thanks are due to A-Xing Zhu, Department of Geography, University of Wisconsin, for numerous discussions and his general advice. Thanks for the constructive reviewers' comments.

Author Contributions

Danlu Cai, Yanning Guan and Shan Guo contributed to the design, development and evaluation of the proposed methodology; Danlu Cai and Chunyan Zhang contributed to the IDL program based methodology processes; Danlu Cai and Klaus Fraedrich contributed to the structure arrangement and detailed writing of the manuscript.

Conflicts of Interest

The authors declare no conflict of interest.

Reference

1. Smith, T.T.M.; Shugart, H.H.; Woodward, F.I. *Plant Functional Types: Their Relevance to Ecosystem Properties and Global Change*; Cambridge University Press: Cambridge, UK, 1997; Volume 1, p. 388.

2. Parry, M.L. *Climate Change 2007: Impacts, Adaptation and Vulnerability*; Cambridge University Press: Cambridge, UK, 2007; Volume 4, p. 986.
3. Bonan, G.B.; Levis, S.; Kergoat, L.; Oleson, K.W. Landscapes as patches of plant functional types: An integrating concept for climate and ecosystem models. *Global Biogeochem. Cy.* **2002**, *16*, doi:10.1029/2000GB001360.
4. Strahler, A.; Muchoney, D.; Borak, J.; Friedl, M.; Gopal, S.; Lambin, E.; Moody, A. *MODIS Land Cover Product, Algorithm Theoretical Basis Document (ATBD) Version 5.0*; Boston University: Boston, MA, USA, 1999.
5. Lapola, D.M.; Oyama, M.D.; Nobre, C.A.; Sampaio, G. A new world natural vegetation map for global change studies. *Anais da Academia Brasileira de Ciencias* **2008**, *80*, 397–408.
6. Representing a New MODIS Consistent Land Surface in the Community Land Model (CLM 3.0). Available online: <http://onlinelibrary.wiley.com/doi/10.1029/2006JG000168/abstract> (accessed on 14 February 2014).
7. Poulter, B.; Ciais, P.; Hodson, E.; Lischke, H.; Maignan, F.; Plummer, S.; Zimmermann, N. Plant functional type mapping for earth system models. *Geosci. Model Dev. Discuss.* **2011**, *4*, 2081–2121.
8. Verant, S.; Laval, K.; Polcher, J.; de Castro, M. Sensitivity of the continental hydrological cycle to the spatial resolution over the Iberian Peninsula. *J. Hydrometeorol.* **2004**, *5*, 267–285.
9. Sun, W.; Liang, S.; Xu, G.; Fang, H.; Dickinson, R. Mapping plant functional types from MODIS data using multisource evidential reasoning. *Remote Sens. Environ.* **2008**, *112*, 1010–1024.
10. Friedl, M.A.; Brodley, C.E.; Strahler, A.H. Maximizing land cover classification accuracies produced by decision trees at continental to global scales. *IEEE Trans. Geosci. Remote Sens.* **1999**, *37*, 969–977.
11. Hansen, M.; Dubayah, R.; DeFries, R. Classification trees: An alternative to traditional land cover classifiers. *Int. J. Remote Sens.* **1996**, *17*, 1075–1081.
12. Sun, W.; Liang, S. Methodologies for Mapping Plant Functional Types. In *Advances in Land Remote Sensing*; Springer: New York, NY, USA, 2008; pp. 369–393.
13. Lhermitte, S.; Verbesselt, J.; Verstraeten, W.W.; Coppin, P. A comparison of time series similarity measures for classification and change detection of ecosystem dynamics. *Remote Sens. Environ.* **2011**, *115*, 3129–3152.
14. Andres, L.; Salas, W.; Skole, D. Fourier analysis of multi-temporal AVHRR data applied to a land cover classification. *Int. J. Remote Sens.* **1994**, *15*, 1115–1121.
15. Lhermitte, S.; Verbesselt, J.; Jonckheere, I.; Nackaerts, K.; van Aardt, J.; Verstraeten, W.; Coppin, P. Hierarchical image segmentation based on similarity of NDVI time series. *Remote Sens. Environ.* **2008**, *112*, 506–521.
16. Geerken, R.; Zaitchik, B.; Evans, J.P. Classifying rangeland vegetation type and coverage from NDVI time series using Fourier Filtered Cycle Similarity. *Int. J. Remote Sens.* **2005**, *26*, 5535–5554.
17. Evans, J.; Geerken, R. Classifying rangeland vegetation type and coverage using a Fourier component based similarity measure. *Remote Sens. Environ.* **2006**, *105*, 1–8.
18. Geerken, R.A. An algorithm to classify and monitor seasonal variations in vegetation phenologies and their inter-annual change. *ISPRS J. Photogramm.* **2009**, *64*, 422–431.

19. Azzali, S.; Menenti, M. Mapping vegetation-soil-climate complexes in southern Africa using temporal Fourier analysis of NOAA-AVHRR NDVI data. *Int. J. Remote Sens.* **2000**, *21*, 973–996.
20. Asrar, G.; Fuchs, M.; Kanemasu, E.; Hatfield, J. Estimating absorbed photosynthetic radiation and leaf area index from spectral reflectance in wheat. *Agron. J.* **1984**, *76*, 300–306.
21. Myneni, R.B.; Hall, F.G.; Sellers, P.J.; Marshak, A.L. The interpretation of spectral vegetation indexes. *IEEE Trans. Geosci. Remote Sens.* **1995**, *33*, 481–486.
22. Carlson, T.N.; Ripley, D.A. On the relation between NDVI, fractional vegetation cover, and leaf area index. *Remote Sens. Environ.* **1997**, *62*, 241–252.
23. USGS Shuttle Radar Topography Mission. Available online: <http://glcf.umd.edu/data/srtm/> (accessed on 14 February 2014).
24. Valeriano, M.M.; Kuplich, T.M.; Storino, M.; Amaral, B.D.; Mendes, J.N., Jr.; Lima, D.J. Modeling small watersheds in Brazilian Amazonia with shuttle radar topographic mission-90 m data. *Comput. Geosci.* **2006**, *32*, 1169–1181.
25. Ren, G.; Zhu, A.; Wang, W.; Xiao, W.; Huang, Y.; Li, G.; Li, D.; Zhu, J. A hierarchical approach coupled with coarse DEM information for improving the efficiency and accuracy of forest mapping over very rugged terrains. *Forest Ecol. Manag.* **2009**, *258*, 26–34.
26. Zhang, X.; Sun, S.; Yong, S.; Zhou, Z.; Wang, R. *Vegetation Map of the People's Republic of China (1: 1000000)*; Geological Publishing House: Beijing, China, 2007; p. 1228. (In Chinese)
27. Gao, Q.Z.; Wan, Y.F.; Xu, H.M.; Li, Y.; Jiangcun, W.Z.; Borjigidai, A. Alpine grassland degradation index and its response to recent climate variability in Northern Tibet, China. *Quatern. Int.* **2010**, *226*, 143–150.
28. Liu, Z.; Yang, J.; Chang, Y.; Weisberg, P.J.; He, H.S. Spatial patterns and drivers of fire occurrence and its future trend under climate change in a boreal forest of Northeast China. *Global Change Biol.* **2012**, *18*, 2041–2056.
29. Kalaitzidis, C.; Heinzl, V.; Zianis, D. A Review of Multispectral Vegetation Indices for Biomass Estimation, Imaging Europe. In Proceedings of the 29th Symposium of the European Association of Remote Sensing Laboratories, Chania, Greece, 15–18 June 2009; p. 201.
30. Woodcock, C.E.; Gopal, S. Fuzzy set theory and thematic maps: Accuracy assessment and area estimation. *Int. J. Geogr. Inf. Sci.* **2000**, *14*, 153–172.
31. Tanaka, K.; Tamagawa, I.; Ishikawa, H.; Ma, Y.; Hu, Z. Surface energy budget and closure of the eastern Tibetan Plateau during the GAME-Tibet IOP 1998. *J. Hydrol.* **2003**, *283*, 169–183.
32. Zou, D.; He, Y.; Lin, Q.; Cui, G. Evaluation of the level of threat and protective classification of the vegetation of Makehe Forest in Sanjiangyuan Nature Reserve, west China. *Front. For. China* **2007**, *2*, 179–184.
33. Piao, Y.; Yan, B.; Guo, S.; Guan, Y.; Li, J.; Cai, D. Change Detection of MODIS Time Series Using a Wavelet Transform, Systems and Informatics (ICSAI). In Proceedings of 2012 International Conference 2012, New Jersey, NJ, USA, 16 May 2012; Institute of Electrical and Electronics Engineers: New Jersey, NJ, USA, 2012; pp. 2093–2097.
34. Gitelson, A.A. Wide dynamic range vegetation index for remote quantification of biophysical characteristics of vegetation. *J. Plant Physiol.* **2004**, *161*, 165–173.

35. Rodrigues, A.; Marcal, A.; Furlan, D.; Ballester, M.; Cunha, M. Land cover map production for Brazilian Amazon using NDVI SPOT VEGETATION time series. *Can. J. Remote Sens.* **2013**, *39*, 277–289.
36. Rodrigues, A.; Marcal, A.R.; Cunha, M. Identification of potential land cover changes on a continental scale using NDVI time-series from SPOT VEGETATION. *Int. J. Remote Sens.* **2013**, *34*, 8028–8050.
37. Foody, G.M. Status of land cover classification accuracy assessment. *Remote Sens. Environ.* **2002**, *80*, 185–201.

© 2014 by the authors; licensee MDPI, Basel, Switzerland. This article is an open access article distributed under the terms and conditions of the Creative Commons Attribution license (<http://creativecommons.org/licenses/by/3.0/>).